Comprehensive investigation of buckling behavior of plates considering effects of holes

Behzad Mohammadzadeh[**1], Eunsoo Choi[*1] and Woo Jin Kim[2]

[1]*Department of Civil Engineering, Hongik University, Seoul 04066, Republic of Korea*
[2]*Department of Materials Science and Engineering, Hongik University, Seoul 04066, Republic of Korea*

Abstract. A comprehensive study was provided to investigate the buckling behavior of the steel plates with and without through-thickness holes subjected to uniaxial compression using ABAQUS. The method was validated by the results reported in the literature. Using the critical stresses, the buckling coefficients (K_c) were calculated. The effects of inclusion of material nonlinearity, plate thickness (t), aspect ratio (AR), and initial imperfection on buckling resistance of the plate was studied. Besides, the effects of having the hole in the plate were also studied. The diameter of the hole was normalized by dividing by plate breadth and was given in the form of α. Results showed that perforating one hole in the center of a plate increases the plate buckling resistance while the having two holes resulted in a decrease in the plate buckling resistance. The effects of hole eccentricity (Ecc) on the buckling resistance of the plate was studied. The position of the hole center was normalized by half of the plate breadth and length in X- and Y-directions, respectively. In this study, four cases of boundary conditions were considered, and the corresponding buckling behavior were studied combined with plate aspect ratio. It was observed that the boundary condition of the case I resulted in the highest buckling resistance. Finally, a comparison was made between the buckling behavior of the uniaxially and biaxially loaded plate. It was revealed that the buckling resistance of a biaxially loaded plate is lower half than half of that of the uniaxially loaded plate.

Keywords: buckling analysis; post-buckling; plates; through-thickness hole; buckling coefficient; material nonlinearity; geometrical nonlinearity; hole eccentricity

1. Introduction

One of the structural components which have been widely employed in industries and constructions is the plate (Mohammadzadeh and Noh 2017, Mohammadzadeh and Noh 2015, Kim *et al.* 2018). The structural stability analysis (SSA) has attracted many attentions as an important and interesting subject (Kaci *et al.* 2018, Aghazadeh *et al.* 2018, El-Hania *et al.* 2017, Mohammadzadeh *et al.* 2012, Mohammadzadeh and Noh 2014). One of the important factors causing the instability of plates and columns, and beams is buckling (Musa 2016, Mohammadzadeh and Noh 2016, Choi *et al.* 2018, Ziane, *et al.* 2015, Akbas 2014). Several parameters affect the buckling of the plates among which boundary conditions (BC) and plate thickness (t) have the most important effects on the buckling load (BL) (Chaies 1974, Timoshenko and Gere 2010, Sadamoto *et al.* 2017, Mohammadzadeh and Noh 2014). Despite having several studies of the buckling of plates with respect to various parameters such as BC and loading cases, the effect of in-plane BC on the buckling behavior of plates have been rarely studied (Parajapat *et al.* 2015, Nguyen *et al.* 2017,

Xie *et al.* 2017, Kasaeian *et al.* 2012). Some studies investigated the buckling behavior of the full and partial in-plane restrained plates loaded in compression, bending and shear, numerically and analytically (Bedair and Sherbourne 1994, Ruocco *et al.* 2017, Bedair 1997, Xinwei and Zhangxian 2018). The results showed that considering in-plane BC along the unloaded edges causes a lower F_b and a different mode shape than the plate under free in-plane edge movement.

Some studies investigated the thermal buckling of different type of plates considering a variety of BCs, loading patterns, theoretically and numerically. Bouderba *et al.* (2016) presented a developed FSDT for thermal buckling of FG sandwich plates considering various BCs. Having only four unknowns made the method more simple than conventional FSDT. The results proved that the method can predict the buckling of sandwich plates as accurate as the conventional FSDT. Bousahla *et al.* (2016) presented a four-variable refined plate theory (RPT) to investigate buckling of FGM plates subject to uniform, linear and nonlinear temperatures varying through the h. A parabolic distribution as considered for the transverse shear strains which could satisfy the zero traction BCs on the surfaces of the plate without using shear correction factor (SCF). Menasria *et al.* (2017) proposed an HSDT method which by using a new displacement field provided a simple tool for investigating thermal buckling of FG sandwich plates. They considered uniform, linear and nonlinear temperatures rising through the '*t*'. Chikh *et al.* (2017),

---

∗Corresponding author, Professor
 E-mail: eunsoochoi@hongik.ac.kr
∗∗Ph.D.
 E-mail: Behzad.alb@gmail.com

investigated the thermal buckling of cross-ply composite laminates through a simplified HSDT comprising only four unknowns. The results showed that the method can predict the thermal buckling of composite laminates as accurate as conventional HSDT. Khetir *et al.* (2017), investigated thermal buckling of nanosized FG nano-plates resting on two-parameter elastic foundation under various type of thermal environments by presenting and employing a new trigonometric SDF. The gradual variation of material characteristics in the plane-normal direction *(t)* of the plate was modeled by employing the Mori-Tanaka model. Nonlocal elasticity theory of Eringen was used for capturing the effects of size on buckling characteristics.

Some studies developed theoretical approaches for the investigation of nonlinear post-buckling of various type of plates and beams based on SDF and HSDT (Hichem *et al.* 2017, Abdelaziz *et al.* 2017, Ait Amar Meziane *et al.* 2014, Yazid *et al.* 2018). However, few studies dealt with the investigation of buckling of plates with through-thickness holes. The influences of perforating plate and plate aspect ratio (AS) on the buckling were studied during past years. C.Scheperboer *et al.* (2016), investigated the effects of multiple holes on local buckling (LB) of aluminum and steel plates. They considered slender plates with 1-25 holes subject to compressive load. The results showed that holes had not a significant effect for the case of Euler load, but they affected the failure of the plate substantially. The perforation had a similar effect, in the case of failure load, for both aluminum and steel plates. Some studies investigated the axial buckling of perforated plates (Seifi *et al.* 2017, Jiao *et al.* 2018, Kim *et al.* 2015, Komur and Sonmez 2015), shear buckling of plates and thin-walled shells (Soares and Palermo 2017, Pham 2017, V.Degtyarev and V.Degtyareva 2017), tension buckling of plates with hole (Shimizu 2007, Sweedan and Sawy 2011), and elastic buckling of thin plates with holes in compression or bending (Komur 2011, Guo 2014, Jana 2016, Aykac 2016).

The effect of size and position of circular cut-outs in simply supported (SS) and clamped plates subjected to uniaxial and biaxial compressive loadings and pure shear was studied by Sabir and Chow (1986). El-Sawy and Nazmy (2001) studied the effect of AS on elastic buckling of SS plates with eccentric cut-outs. It was concluded that the buckling behavior in terms of F_b and mode shapes of perforated rectangular plates may not necessarily be the same as that of the perforated square plates. The recommendation of that study was to provide a cut-out in a pre-determined location to avoid a drastic reduction in F_b. Kim, *et al.* (2015) performed a series of numerical studies to analyze the buckling and ultimate strength of reinforced perforated plates. They developed the design formula for calculation of the ultimate strength of the perforated plates. Besides, they proposed an optimum reinforcement method for perforated plates with respect to the loading conditions. Maiorana *et al.* (2009), investigated the effect of the position of circular and rectangular holes on the elastic stability of SS rectangular plates. They considered in-plane compression together with the bending moment for presenting the best orientation of a hole in a plate. Tajdari *et al.* (2011) employed a numerical method through FEM to
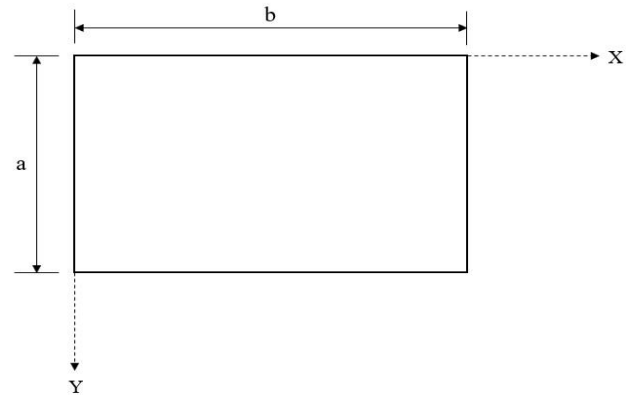

Fig. 1 Illustration of the typical plate

investigate the effects of in-plane BC, AR and hole size on the plate buckling strength.

Majority of studies noted in the literature released the in-plane movements and only considered the out-of-plane BCs for investigating the buckling behavior of the plate. A few studies investigated the effect of in-plane BCs on the plate buckling and were limited to the unloaded edges of the plate. Furthermore, most of them considered one or two specific parameters for investigating the plate buckling behavior, only. Therefore, the interactive effects of different parameters such as *t*, *AS*, hole size (α), and hole Ecc which, in practice, may apply together were not considered. Besides, the K_c which can be employed to calculate the critical F_b of plates were rarely investigated and reported.

Considering the works studied in the literature and the lack of knowledge of buckling behavior of plates with and without holes, motivated this study to provide a comprehensive study to investigate the buckling behavior of the plates with and without holes considering various important parameters which highly affect the plate buckling and give a detailed complete view to readers about the buckling-based failure of plates. The novelty of the work comes up with considering the effects of different in-plane boundary conditions on the maximum sustainable F_b of the plates with and without holes uniaxially loaded along with its length, to the breadth of the plate while the normal-direction displacement is constrained. In addition, the interactive effects of h, aspect ratio and hole size, and hole Ecc are investigated through parametric studies. To characterize the buckling behavior of the plates with holes, the F_b factor which is the ratio of the F_b of the plate with hole to that of the plate without a hole is defined and employed. The effect of size of the hole on F_b is studied in terms of the ratio of the hole diameter to the plate breadth α. The post buckling behavior of the flat plates with and without holes is also investigated. Besides the effect of consideration of initial imperfection on the buckling behavior of the plates is to be studied. Finally, the K_c of plates with holes are calculated and provided to provide designers by a simple calculation and prediction of the critical F_b of plates under various conditions. Having all above provides a comprehensive novel insight in the buckling behavior of plates considering all effective parameters and their corresponding interactions. It will

provide a good understanding of how perforations and other important parameters affect the buckling resistance of the plate and what should be consider for the design purpose.

2. Buckling analysis

2.1 Definition of the problem

Fig. 1 illustrates a typical plate having the width of a and length of b. For all the analysis in this study, a and b is 500 mm 1000 mm, respectively. The only exception is for the part of generalization of the results for which other values of a and b are considered.

The solution of Gerard and Becker is inconvenient to write in closed form. The general buckling stress for the plate under compression parallel to X-axis, σ_c, is defined as given in Eq. (1) (Mohammadzadeh and Noh 2016)

$$\sigma_c = \eta\bar{\eta}\frac{k\pi^2 E}{12(1-\nu^2)}\left(\frac{t}{a}\right)^2 \qquad (1)$$

where k is the buckling coefficient, η plasticity factor, $\bar{\eta}$ cladding reduction factor, ν elastic Poisson's ratio, 't' thickness of th plate and 'a' is the length of the loaded edge in uniaxial compression. Defining the buckling coefficient, K_c, by multiplying three coefficients, η, $\bar{\eta}$, and k, the Eq. (1) can be rewritten in the form of Eq. (2) which represents the critical buckling stress
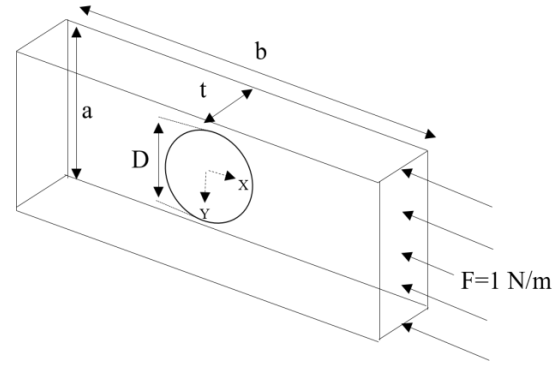
$$\sigma_c = \frac{k_c\pi^2 E}{12(1-\nu^2)}\left(\frac{t}{a}\right)^2 \qquad (2)$$

For the Von Karman's reduced-modulus F_b, it was supposed that the column buckles under a constant load and thus a unique critical load is predicted for a column with respect to the geometrical characteristics and material properties. Shanley (1946) proved that unlike there is no unique critical BL. He resulted that the plastic buckling theory of the column should be reviewed on the basis that buckling occurs simultaneously with an increasing axial load. For analysis of a simply supported plate including material nonlinearity such as plasticity, the equation takes the following form (Johari Moghadam 2015, Grognec and Van 2011, Grognec and Sauod 2015)

$$\sigma_{cp} = \frac{k_p\pi^2 E\sqrt{\eta}}{12(1-\nu^2)}\left(\frac{t}{a}\right)^2 \qquad (3)$$

where $\eta = \frac{E_t}{E}$ is the plasticity factor, E_t tangent modulus regarding the nonlinear behavior of the material and E is the elastic modulus of the material.

In the application of structural members, holes may be perforated in webs or flanges of the member with respect to requirements such as piping, electrical cables, and ducts. Besides, to embed the transverse member, making cutout is needed. Cutouts affect the stiffness and strength of the structural members. The critical stress due to the presence of the hole can be represented by analogous equations regarding uniaxial compression in terms of the respective K_c, namely, K_u^H, as follows

(a) Typical plate with one hole
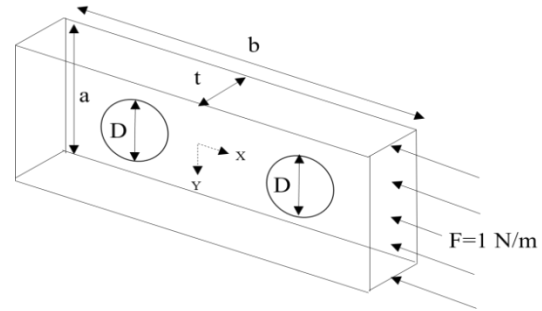
(b) Typical plate with two holes

Fig. 2 Schematic of plates with hole and the applied compressive unit load

$$\sigma_u^H = \frac{K_u^H\pi^2 E}{12(1-\nu^2)}\left(\frac{t}{a}\right)^2 \qquad (4)$$

2.1.1 Consideration of hole

The buckling and post-buckling analyses of a variety of plates with and without through-thickness holes were performed in this study. The aim was to find K_c for each material and specific configuration. Finally, the obtained K_c were generalized to make them practically applicable. For the plates having through-thickness holes, due to their multi-functional application, two cases of one hole and two holes were considered. The compressive unit load was applied to two edges of the plate. In order to have a comprehensive study, we required that consider both thin and thick plates. It is appropriate to note that, considering t as the plate thickness and 'a' as the smallest side of the plate, batch of thin plates covers plates with $t<20a$ while a batch of thick plates covers plates with $t>20b$. Therefore, this study considered a variety of thicknesses for each type of plate to investigate the effects of thickness on buckling of the plates; 1, 2, 3, 4, 5, 10, 15, and 20 mm for the batch of thin plates and 25, 30 and 40 mm for thick plates. For the batch of plates with holes, a geometric parameter $\alpha=d/a$, the ratio of the diameter of the hole to the plate width, was used to determine the critical buckling values for various states. This ratio states that for specific conditions and plate dimensions what size of the hole is permitted to be perforated in the plate. This study considered a range of α from 0.05 to 0.6 to investigate the effects of size of the hole on the buckling stress of plate. It was supposed that, based on previous studies [7,8], when the diameter of a typical hole gets about half of the side of a plate the plate cannot be in a stable
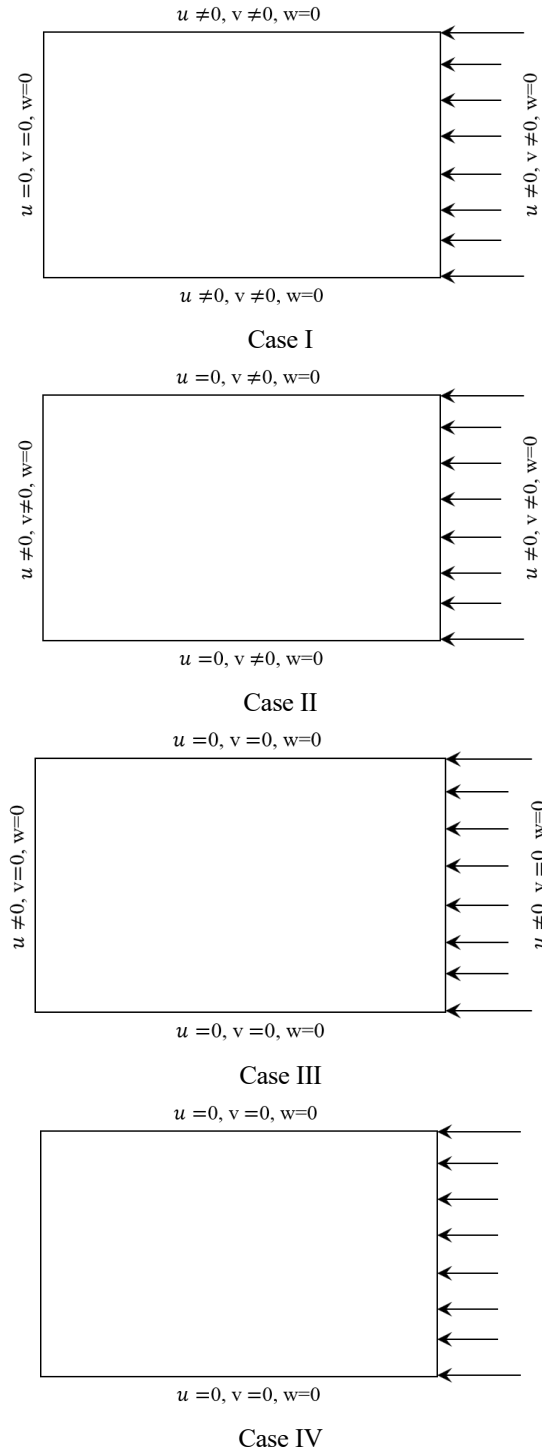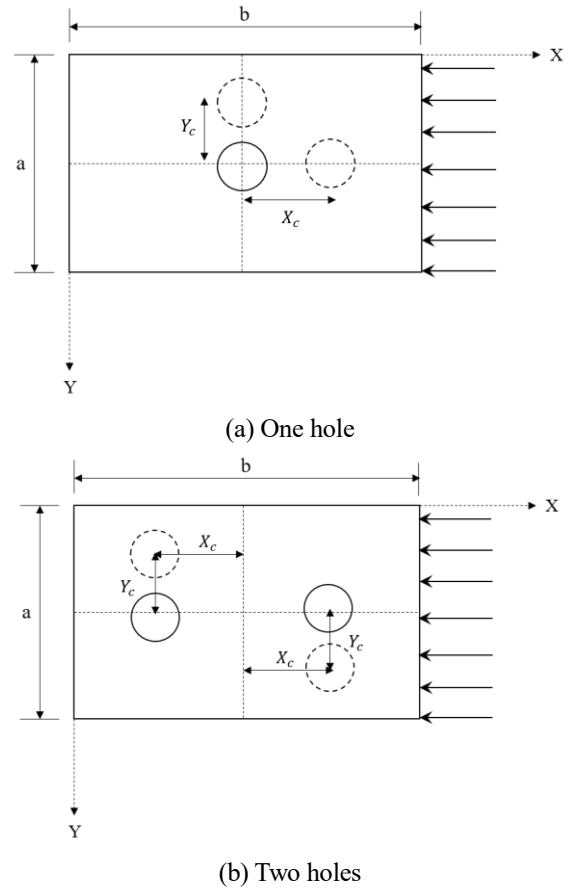
Case I

Case II

Case III

Case IV

Fig. 3 Graphical representation of various cases of boundary conditions

(a) One hole

(b) Two holes

2.1.2 Boundary conditions

This study considers three different cases of in-plane boundary conditions while similar out-of-plane boundary conditions are taken into account for all cases. The mid-surface in-plane displacements in loading direction and transverse direction are represented by u, and v, respectively. The out-of-plane displacement is constrained for all cases. Fig. 3 shows the representation of the boundary conditions.

In the main part of this study, for buckling analysis of the plates, the boundary conditions of the case I is employed. Thereafter, to evaluate the effects of boundary conditions on the buckling behavior of plates with and without holes two other cases are considered as illustrated in Fig. 3. It is appropriate to note that for these analyses, the plates with one hole and two holes with the thicknesses of 5 and 25 mm are considered.

2.1.3 Eccentricity of holes

In order to evaluate the effects of E_{cc} of holes on the F_b of the plate is to be investigated. To evaluate the Ecc in loading direction (X-direction) the F_b is investigated with respect to $\beta = \frac{X_c}{b/2}$ while for the direction transverse to the loading (Y-direction), the F_b is calculated with respect to $\gamma = \frac{Y_c}{a/2}$. Fig. 4 illustrates the Ecc of the holes in the plate. Either one hole or two holes can be considered in the plate. It is notable that, the plates with one hole and two holes with the thicknesses of 5 and 25 mm and AR=0.5 are considered in this part. In order to present the results a Ecc-related buckling load

condition and might fail. Fig. 2 shows the typical plates with holes in which the variation of α and t is illustrated. The origin of the coordinate system is considered at the center of the plate.

In this study, three types of homogeneous steel plates were considered, namely, plates without the hole, with one hole, and with two holes. The buckling and post-buckling analyses of each type were performed and discussed separately as follows.

Table 1 Nonlinear properties of steel

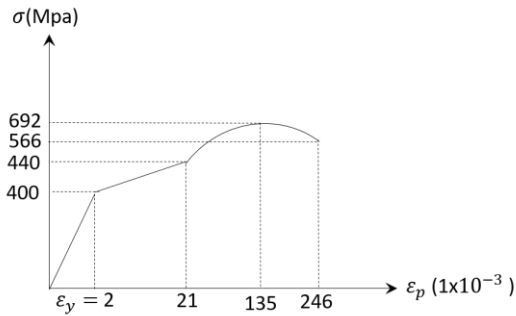| Stress (MPa)	940	1034	1330.1	1626.2
Plastic strain (%)	0.459	5.044	32.5	59.15

Fig. 5 Illustration of nonlinear mechanical properties of steel

ratio, *Fecc*, is presented. *Fecc*, is the ratio of F_b of holes with Ecc to the centroid holes.

2.1.4 Aspect ratio and imperfection

The effects of plate AR, plate breadth to the length, AR= a/b, on its buckling behavior is going to be investigated. In this regard, four ARs were considered for the plate: AR=0.1, 0.25, 0.5, 0.75, and 1. It is appropriate to note that for these analyses, the plates with one hole and two holes with the thicknesses of 5 and 25 mm are considered.

Sometimes there is already initial imperfection in the plate due to some reasons such as manufacturing process or installation in a structure. Therefore, this study investigated the effects of having an initial imperfection on the plate buckling resistance. The initial imperfection was considered in the form of a ratio of the central displacement to the plate thickness, $\frac{\delta}{t}$. The plate of 5 mm thickness with and without holes were considered for $0.1 \le \frac{\delta}{t} \le 0.6$. The boundary condition of the case I and AR=0.5, were attributed to the plate. The The diameter to the plate width ratio of α=0.2 was adopted for the holes.

2.2 Steel plate mechanical properties

The mechanical elastic properties of the structural steel include the Poisson's ratio of 0.3, a modulus of elasticity of 210 GPa and yield stress of 400 MPa. The steel nonlinear mechanical properties are provided in Table. 1 and illustrated in Fig. 5 in the form of the stress and strain relation.

2.3 Finite element modeling

The finite element method (FEM) was employed to do buckling and post-buckling analyses. FEM is a numerical approach which approximates solutions of governing partial differential equations. To have more concise modeling and results, three elements were considered through the thickness of the plate. It provides more information about displacements in the plane-normal direction.
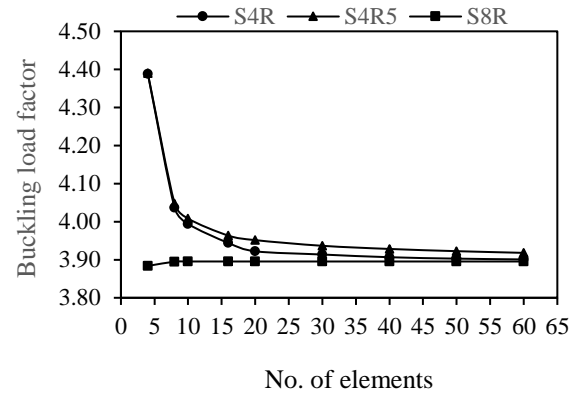
(a) Plate without hole
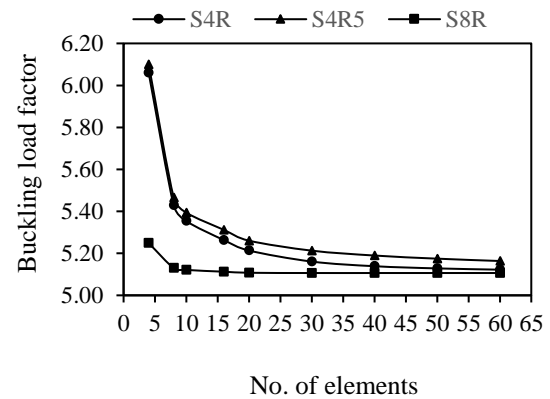
(b) Plate with one hole
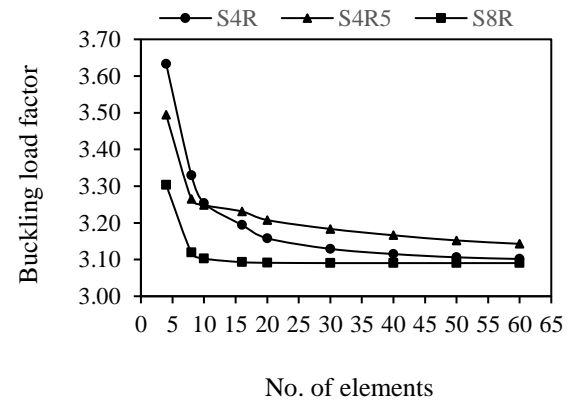
(c) Plate with two holes

Fig. 6 Comparative graph presenting the efficiency of different shell elements on convergence

2.3.1 Mesh description

The library of ABAQUS consists of three categories, namely, general-purpose, thin, and thick shell elements. The batch of thin shell elements provide solutions to the shell-related problems, the batch of thick shell elements results in solutions for structures modeled by the Mindlin shell theory, and general-purpose shell elements can be used for both thin and thick shell problems. The general-purpose shell elements can be the first choice for structural analysis. However, for specific applications, it may be possible to obtain enhanced performance by choosing one of the thin or thick shell elements. Second-order elements provide higher accuracy than first-order elements. They capture stress

concentrations more effectively and are better for modeling geometric features. In order to make element stiffness full-integration, and reduced-integration elements, are available in Abaqus. Reduced integration reduces running time, so, it is adopted to model and mesh the plate.

In order to choose the most appropriate shell element, the convergence rate of different shell elements was studied by making a comparison between the F_b factor obtained for different element types and mesh size. For this aim, three types of plates of 500 mm width, 1000 mm length, and 10 mm thickness were considered: a plate without a hole, a plate with a hole of 300 mm diameter, and a plate with two holes of 300 mm diameter. Three types of shell elements were considered to be investigated: S4R, a 4-node doubly curved thin or thick shell with reduced integration, S4R5, a 4-node doubly curved thin shell with reduced integration, and S8R, an 8-node doubly curved thick shell with reduced integration. Fig. 6 illustrates the comparative graphs presenting the convergence of the load buckling factor, which is the ratio of the F_b of the plate with hole to the that of plate without a hole (theoretical F_b), with respect to the type of element and mesh size.

As can be seen from Fig. 6, the S8R showed the best computational efficiency and convergence rate among all. It is notable that, the convergence was obtained for the mesh size corresponding to 20 elements along with the breadth of the plate. Therefore, to model and mesh the plates the quadratic eight-node doubly curved thick shell elements (S8R) using six degrees-of-freedom, and reduced integration was employed. The element S8R is adopted due to its sufficiency compared to other elements available in Abaqus [13]. To mesh the plate, 10 elements were considered along with the breadth of the plate.

2.3.2 Post-buckling analysis

Buckling is a form of sudden failure when the compressive load is applied to a structure. The post-buckling stage is a continuation of the buckling stage. After a load gains its critical value, it may begin to decrease, or experiences no change, while deformation keeps increasing. Sometimes, the structure continues to take more load after a certain amount of deformation, to continue increasing deformation which eventually results in a second buckling cycle. By performing post-buckling analysis more information, about the structural behavior, than linear eigenvalue analysis can be obtained. It includes geometrical nonlinearity and material nonlinearity. Geometric nonlinearity occurs due to small and large strains, rotations and deficiency of structural stability. Material nonlinearity comes from time-independent material behavior such as plasticity and time-dependent material behavior such as creep and viscoelasticity.

3. Results and numerical investigations

3.1 Verification

The numerical analysis using commercially available finite element package ABAQUS considered in this study is to be verified by calculating the buckling load ratio (F_{br}),

Table 2 Comparison between F_b ratios of this study and Ko (1998) (plates with one hole)

Study	α =0.2		α =0.5	
	AR=0.5	AR=1	AR=0.5	AR=1
Present	1.05	0.95	1.07	0.93
Ko (1998)	1.01	0.99	1.02	0.98
Error (%)	3.81	4.01	4.67	5.10

Table 3 F_{bc} and stresses of plates with one hole considering thicknesses and α

α (d/a)	Thickness (mm)											
	5		10		20		25		30		40	
	F_{bc} (N)	σ_c (MPa)	F_{bc} (N)	σ_c (MPa)	F_{bc} (N)	σ_c (Mpa)	F_{bc} (N)	σ_c (Mpa)	F_{bc} (N)	σ_c (MPa)	F_{bc} (N)	σ_c (Mpa)
0	372.77	74.6	2957.4	295.7	23194	1159.7	44787	1791.5	76442	2548.1	176311	4407.8
0.05	373.89	74.8	2965.9	296.6	23259	1163.0	44909	1796.4	76646	2554.9	176763	4419.1
0.1	377.04	75.4	2990.4	299.0	23443	1172.2	45259	1810.4	77233	2574.4	178060	4451.5
0.2	388.72	77.7	3081.6	308.2	24132	1206.6	46559	1862.4	79401	2646.7	182822	4570.6
0.3	406.57	81.3	3220.1	322.0	25167	1258.4	48507	1940.3	82634	2754.5	189829	4745.7
0.4	422.56	84.5	3348.4	334.8	26151	1307.6	50341	2013.6	85604	2853.5	195630	4890.8
0.5	449.03	89.8	3549.4	354.9	27564	1378.2	52891	2115.6	89621	2987.4	203126	5078.2
0.6	492.15	98.4	3877.5	387.8	29865	1493.3	57000	2280.0	95968	3198.9	213931	5348.3

Table 4 Critical buckling coefficients of plates with one hole considering thicknesses and α

α (d/a)	Thickness (mm)					
	5	10	20	25	30	40
0	3.93	3.90	3.82	3.78	3.73	3.63
0.05	3.94	3.91	3.83	3.79	3.74	3.64
0.1	3.97	3.94	3.86	3.82	3.77	3.66
0.2	4.10	4.06	3.97	3.92	3.87	3.76
0.3	4.28	4.24	4.14	4.09	4.03	3.91
0.4	4.45	4.41	4.31	4.24	4.18	4.03
0.5	4.73	4.68	4.54	4.46	4.37	4.18
0.6	5.19	5.11	4.92	4.81	4.68	4.40

the ratio of the F_b of plate with the hole to that of the plate without a hole obtained theoretically from Timoshenko and comparing them with the results reported in the literature (Ko 1998). For this aim, a simply supported plate in the out-of-plane direction subjected to uniaxial compression was considered. The analysis was done for plates utilizing the AR= 0.5, 1 and for α =0.2, 0.5. The comparison between the estimation of the buckling load ratio, F_{br}, of the plates having a hole at the center obtained in this study and those given in Ko (1998) is provided in Table 2.

Taking look at the results given in Table 2, a good agreement was achieved between the results of this study and the results given in the literature.

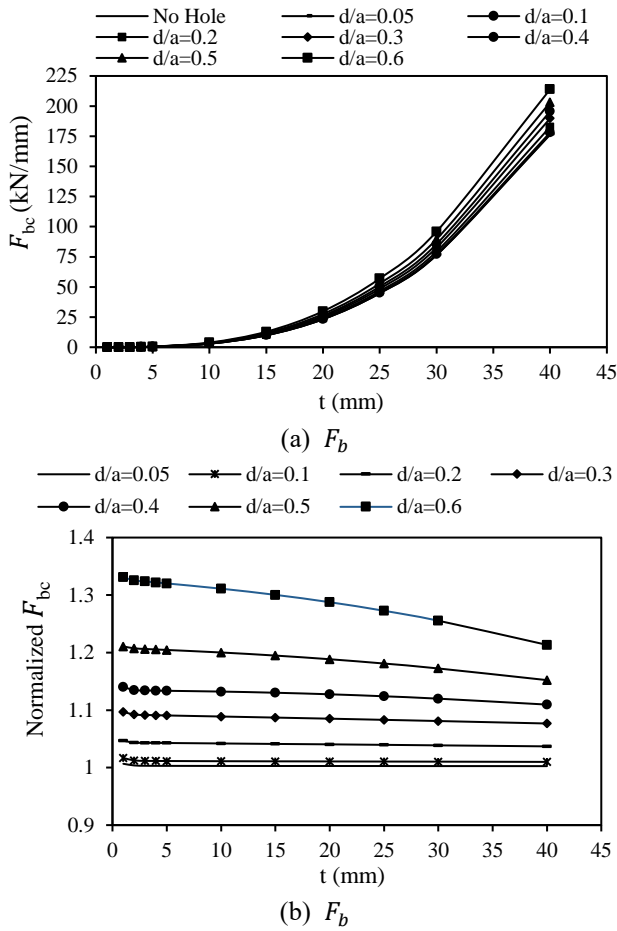### 3.2 Uniaxial compression

3.2.1 Plate thickness and hole size effects

(a) F_b

(b) F_b

Fig. 7 Variation of F_b and normalized F_b with respect to the plate thickness

Table 5 F_{bc} and σ_c of plates with two holes considering thicknesses and α

α (d/a)	Thickness (mm)											
	5		10		20		25		30		40	
	F_{bc} (N/mm)	σ_c (MPa)	F_{bc} (N/mm)	σ_c (MPa)	F_{bc} (N/mm)	σ_c (MPa)	F_{bc} (N/mm)	σ_c (MPa)	F_{bc} (N/mm)	σ_c (MPa)	F_{bc} (N/mm)	σ_c (MPa)
0	372.77	74.6	2957.4	295.7	23194	1159.7	44787	1791.5	76442	2548.1	176311	4407.8
0.05	369.4	73.9	2930.6	293.1	22985	1149.3	44385	1775.4	75759	2525.3	174764	4369.1
0.1	360.53	72.1	2859.6	286.0	22427	1121.4	43311	1732.4	73935	2464.5	170611	4265.3
0.2	337.12	67.4	2672.9	267.3	20954	1047.7	40461	1618.4	69067	2302.2	159398	3985.0
0.3	321.2	64.2	2544.2	254.4	19904	995.2	38397	1535.9	65480	2182.7	150836	3770.9
0.4	316.98	63.4	2505.1	250.5	19502	975.1	37522	1500.9	63815	2127.2	146162	3654.1
0.5	314.83	63.0	2476.8	247.7	19094	954.7	36544	1461.8	61814	2060.5	139957	3498.9
0.6	299.98	60.0	2346.8	234.7	17884	894.2	34024	1361.0	57198	1906.6	127894	3197.4

Table 6 Critical buckling coefficients of plates with one hole considering thicknesses and α

α (d/a)	Thickness (mm)					
	5	10	20	25	30	40
0	3.93	3.90	3.82	3.78	3.73	3.63
0.05	3.89	3.86	3.78	3.74	3.70	3.60
0.1	3.80	3.77	3.69	3.65	3.61	3.51
0.2	3.55	3.52	3.45	3.41	3.37	3.28
0.3	3.38	3.35	3.28	3.24	3.19	3.10
0.4	3.34	3.30	3.21	3.16	3.11	3.01
0.5	3.32	3.26	3.14	3.08	3.02	2.88
0.6	3.16	3.09	2.94	2.87	2.79	2.63

The critical buckling loads (F_{bc}) and corresponding stresses obtained from analyses of plates with and without holes to which a variety of thickness values were specified. In the first step, the buckling behavior and later the post-buckling behavior of plates were investigated.

a. Plates with one hole

To investigate the buckling behavior and finding the F_{bc}, a load of unit value was applied to the breadth of the plate. When the applied load reaches the critical F_{bc}, the plate cannot provide an appropriate structural function and fails. Therefore, having the plate F_b is a key parameter of the design of plated structures, especially, those subjected to compressive loads. Table 3 provides F_{bc} of plates with 5, 10, 20 mm, for the batch of thin plates, and 25, 30, 40 mm for the batch of thick plates. A range of holes with α from 0.05 to 0.6 were considered in the middle of plate. Table the 4 provides the corresponding K_c.

The variation of F_{bc} with respect to thickness is illustrated in Fig. 7(a). To provide a better understanding of the buckling behavior of the plates with a through-thickness hole, the critical F_b of each plate was normalized with dividing by F_b of the plate with the same thickness and no hole. The variation of the normalized F_b with respect to '*t*' is illustrated in Fig. 7(b).

As can be seen from the Fig. 7(a), as the plate thickness increased, the critical F_b also increased. Results showed that the lowest critical loads were obtained for the plate without hole while the highest critical load obtained for the plate with a hole of *d/a*=0.6. The variation of normalized bucking load with respect to plate thickness shown in Fig. 7(b) shows that for each hole size, the normalized F_b of the plates decreased with increasing the thickness. For thinner plates, the ratios of the F_{bc} of the plate with a hole to the plate with no hole are higher than those of thick plates.

b. Plates with two holes

The effects of perforating two holes through the plate on its buckling resistance were investigated. Centers of the two holes were placed at the points with coordinates of X=-250 mm, Y=0, and X=250 mm, Y=0. The same range of α, which determine the size of holes, was considered: 0.05< α < 0.6. For the thickness of the plate, similar values to those of plates having one hole were considered. The obtained F_{bc} are given in Table 5. The corresponding K_c are provided in Table 6. In order to provide a good insight into the buckling behavior of the plates with two holes, the variation of F_b with respect to h is illustrated in Fig. 8(a) while the variation of normalized F_b with respect to h is provided in Fig. 8(b).

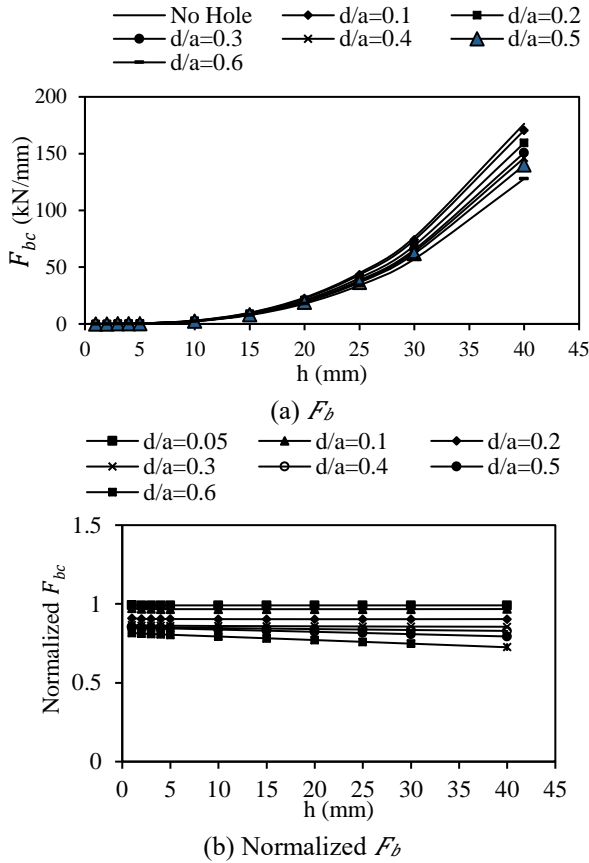*3.2.2 Boundary conditions and aspect ratio*

(a) F_b

(b) Normalized F_b

Fig. 8 Variation of F_{bc} and normalized F_{bc} with respect to the h

(a) Plate with one hole ($\alpha=0.6$)

(b) Plate with two holes ($\alpha=0.6$)

(c) Plate with one hole ($\alpha=0.2$)

(d) Plate with two holes ($\alpha=0.2$)

Fig. 9 Variation of F_{hn} with respect to AR and for $\alpha=0.2$, and 0.6

The effects of different boundary conditions on buckling behavior of the plates were investigated. For this aim, plates of 500 mmm breadth and 1000 mm length with thicknesses of 5 and 25 mm were considered. Plates with holes having the ratio of hole diameter to the plate breadth of $\alpha=0.2$, and 0.6 were considered for the analyses. The K_c of plates with holes were normalized through dividing by K_c of plates without holes (F_{hn}). The variation of normalized K_c with respect to AR is presented in the form of comparative graphs as given in Fig. 9.

3.2.3 Eccentricity

The effects of hole Ecc on the buckling behavior of plates with AR=0.5 and thicknesses of 5, and 25 mm with one hole and two holes were considered. The diameter to breadth ratio of $\alpha=0.2$ was adopted to perforate holes on the plate. The results are presented in the form of Ecc-related buckling load factor, F_{ecc}, versus $\beta = \frac{x_c}{b/2}$, and to $\gamma = \frac{y_c}{a/2}$, in x-direction and y-direction, respectively. F_{ecc} is the ratio of the F_b of plate with holes with Ecc to the those of the plate with centroid holes. The effects of hole Ecc on the buckling behavior of plates with one hole, and two holes are illustrated in Figs. 10, and 11, respectively.

3.2.4 Consideration of Initial imperfection

The effects of initial imperfection on the buckling resistance of the plate were investigated and reported in the form of graphs illustrating the variation of F_{hn}, the ratio of
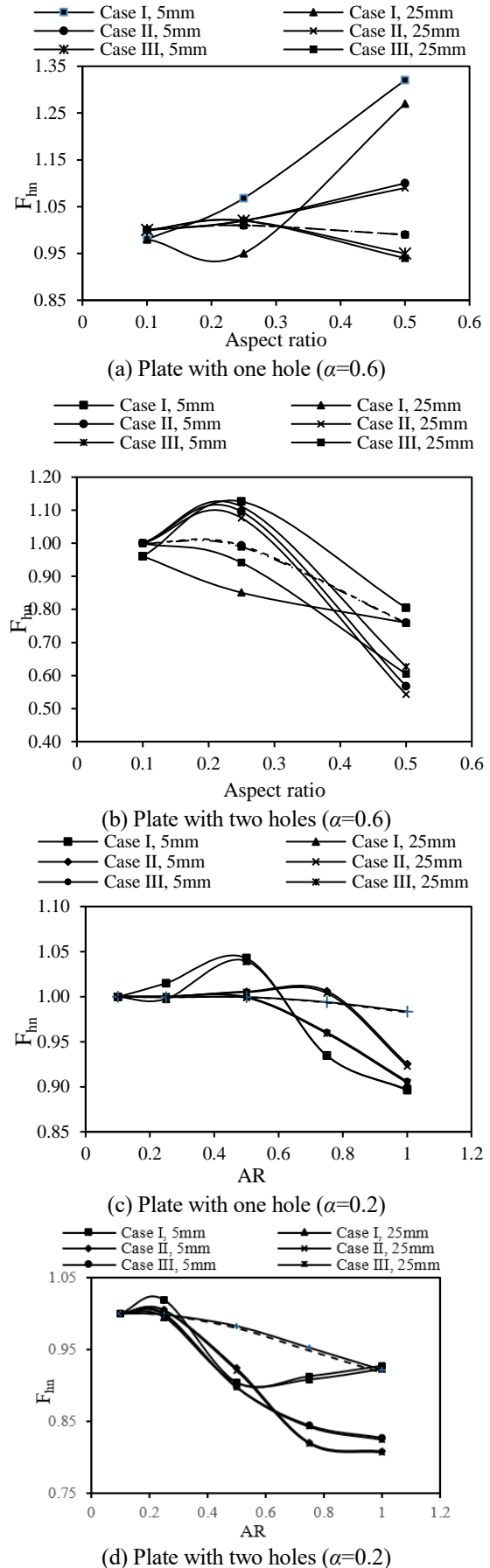
(a) X- direction

(b) Y-direction

Fig. 10 Variation of F_b for plates of 5 mm thickness with one hole with respect to β, and γ

(a) Same orientation

(b) Opposite orientation
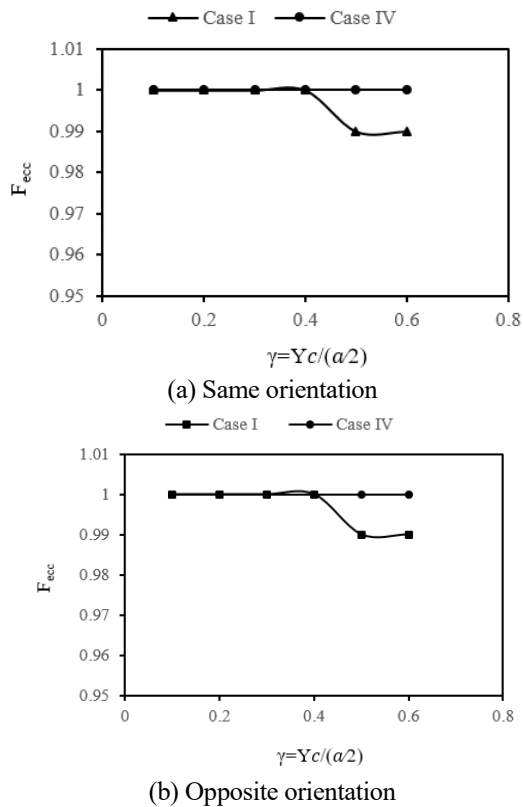
Fig. 11 Variation of F_b for plates of 5 mm thickness with two holes with respect to γ
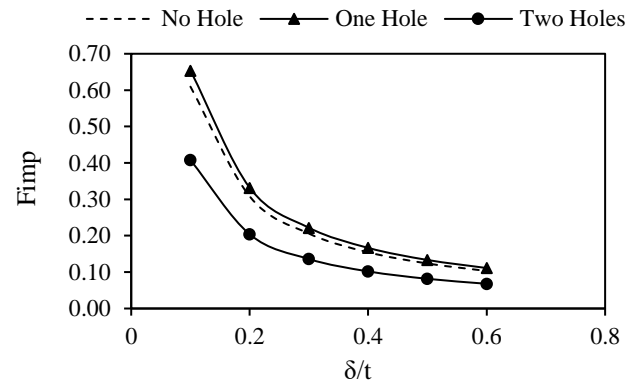

Fig. 12 Variation of buckling resistance of the plates considering the initial imperfections
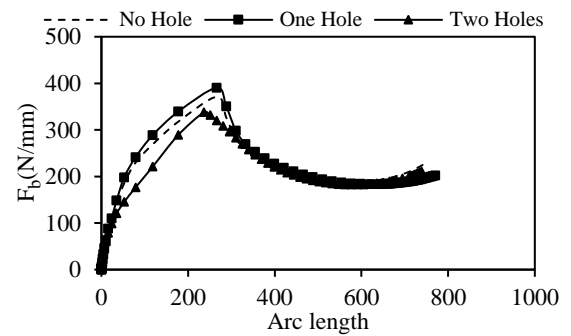
(a) Variation of F_b with respect to arch length

(b) Variation of F_b versus out-of-plane displacement (U3)

Fig. 13 Post-buckling behavior of plates with and without holes

F_b corresponding to the plates with initial imperfection to the those of plates without imperfection, with respect to the ratio of the imperfection to the plate thickness.

3.2.5 Post-buckling

The post-buckling behavior of the plates with and without holes was studied by employing the Arc-length method (RIKS method) considering the thickness of 5 mm and boundary conditions of the case I and illustrated in Fig. 13 in the form of variation of F_b with respect to arc length (Fig. 13(a)) and with respect to out-of-plane displacement U3 (Fig. 13(b)). The graph with dashed-line shows the post-buckling behavior of the plate without a hole. Solid line with rectangles indicates

Table 7 Comparative table obtained for verifying obtained K_c

Number of holes	Thickness (mm)	$\alpha=d/a$	K_c	ABAQUS Buckling stress (MPa)	Theoretical by K_c Buckling stress (MPa)	Error (%)
One Hole	t=5	0.2	4.10	1862.38	1945.45	4.27
		0.4	4.45	2013.6	2111.53	4.64
		0.6	5.19	2300.0	2462.66	6.6
	t=10	0.2	4.06	7214.3	7705.88	6.38
		0.4	4.41	7926.5	8370.18	5.30
		0.6	5.11	8995.4	9698.78	7.25
Two Holes	t=5	0.2	3.55	1613.5	1684.48	4.21
		0.4	3.34	1506.8	1584.83	4.92
		0.6	3.16	1440.0	1499.96	3.96
	t=10	0.2	3.52	6171.8	6680.96	7.62
		0.4	3.30	5790.0	6236.4	7.56
		0.6	3.09	5500.0	5864.82	6.22

the post buckling behavior of the plate with one hole while the solid line with triangles illustrates the post-buckling behavior of the plates with two holes.

4. Discussions

This study investigated the buckling behavior of the steel plates considering various geometrical parameters like AR, thickness, and discontinuities such as perforations and hole eccentricities. Besides, the effects of different boundary conditions on the buckling resistance of the plate were considered. For the analysis, the commercially available finite element package ABAQUS were employed. The uniaxial compression was applied to one side of the plate. In the first part of this study the critical K_c were calculated and presented. They can be used to calculate the critical buckling stress of a desired steel plate. In order to use them for plates with different ARs the generalization of the presented K_c is required to be studied.

4.1 Generalization of the buckling

In order to investigate the generality of the K_c presented in this study, the plates having the breadth of 100 mm and length of 200 mm considering thicknesses of 1, 3, 5 and 10 mm and $\alpha=0.2$, 0.4, and 0.6, were considered. The analyses were performed using ABAQUS and the corresponding critical stresses were calculated. Then the theoretical critical stresses were calculated by using the presented K_c. Thereafter, the results obtained from FEM analyses and those calculated by K_c were compared and the discrepancies between the two models were reported as given in Table 7.

From the results given in Table 7 it can be concluded that the K_c obtained in this study can be applied to plates having different dimensions but having the same ratio α. The last column of Table 7 shows discrepancies between buckling stresses calculated using presented K_c and those

obtained from FEM analyses through ABAQUS. The calculated errors are small, and good agreement is observed for the results obtained from both FEM and theoretical analyses.

4.2 Comparison

a. Aspect ratio, boundary conditions, thickness, and imperfection

As can be seen from the graphs given in Fig. 9, different trends were obtained for different hole size and numbers of the hole. For the plates with one hole and α=0.6, the F_{hn}, the ratio of the F_b of plate with the hole to that of the plate without a hole, increases with the increase in the plate AR for all cases of boundary conditions except for case III. The best performance and highest buckling resistance were obtained for the boundary condition of the case I and the plate of 5 mm thickness which is categorized in the batch of thin plates. The lowest buckling resistance was observed for the boundary condition of case III. An inverse trend was observed for the plate with one hole and α=0.2. Like the plate utilizing $\alpha=0.6$, the highest K_c was obtained for the case I, while the lowest one observed for case III.

Investigating the buckling behavior of the plates with two holes, similar trends were observed for both *α*=0.2, and 0.6. As the AR increases the F_{hn} decreases. The best performance was achieved for the boundary condition of the case I and thickness of 5 mm while the worst one was obtained for the boundary condition of case III and thickness of 25 mm. From the results it can be concluded that the boundary condition of case I, which constrained the plate in loading direction for all in-plane and out-of-plane displacements and constrained the other sides of the plate for displacement in out-of-plane direction, can be used for the practical applications to provide the best buckling performance for the steel plates with holes.

The study on the effects of plate thickness on F_b of plates showed that by increasing the plate thickness the amount of F_b sustained by the plate increases. The increase in F_b followed a cubic order as shown in Eq. (5).

$$F_2 = F_1 \left(\frac{t_2}{t_1}\right)^3 \tag{5}$$

The results also showed that as the size of the hole increases the buckling resistance of the plate decreases. To provide a better understanding of the effects of hole size on the buckling behavior of the plates the obtained F_b of plates with holes were normalized by dividing by F_b of plate without holes as shown in Fig. 8(b). As can be observed, for a specific size of hole an increase in the plate thickness did not affect the normalized F_b.

The effects of an existent initial imperfection on the buckling resistance of the steel plates also studied. As can be seen from the Fig. 12, by increasing the initial imperfection the buckling resistance of the plate decreased following a nonlinear trend. It holds for all plates with and without a hole.

b. Hole eccentricity and post-buckling

The investigations showed that perforating a hole at the

center of the plate increases the buckling resistance of the plate while having two holes on a plate decreases the critical F_b carried by a plate. The effect of hole *Ecc* on the buckling behavior of the plates were illustrated in Fig. 11. The *Ecc* in X-direction (loading direction) was normalized by dividing by the half of the plate length, $\beta = \frac{x_c}{b/2}$, and in Y-direction (transverse to the loading direction) was normalized by dividing by half of the plate breadth, $\gamma = \frac{y_c}{a/2}$. For plate with one hole the effect of Ecc was studied in both X-and Y-directions while for the plates with two holes it was investigated in Y-direction considering two cases: a) hole positions move in a same orientation, and b) hole positions move in opposite orientation.

The results showed that for the plates with one hole, increasing in Y-direction decreased the buckling resistance of the plate for both boundary conditions of the cases I, and IV. The interesting result was that although previous investigations showed that the boundary condition case I provided the best performance but for the *Ecc* of holes it did not necessarily yield in the best buckling resistance. As can be seen from Fig. 10(a) the boundary condition of case IV showed a higher buckling resistance than case I. The same trend was almost observed for the *Ecc* in X-direction. It is worthy to note that the Ecc in X-direction did not have a significant effect on the buckling resistance of the plate utilizing the boundary condition case IV.

Almost the same trend was observed for two cases of the plates having two holes. As can be seen from Fig. 11 the Ecc had a negligible effect on the buckling resistance of the plate for $\gamma < 0.4$, for both boundary conditions of the case I, and IV. For $\gamma > 0.4$ and boundary condition of the case I a decrease in plate buckling resistance was observed while for the boundary condition of case IV no significant effect was seen. It can be concluded that applying the boundary condition of case IV provides the best buckling performance for any required hole Ecc no matter the buckling resistance of the plate.

The post-buckling behavior of the plates with and without hole having the boundary condition of the case I was illustrated in Fig. 13. The plate with a hole in the center provided the highest buckling resistance until the buckling occurred and plate entered in the phase of instability. Later on, a sudden drop can be seen in the graph which shows a tremendous decrease in the plate buckling resistance. But, it again gained the resistance due to the back pressure which leads to a kind of hardening. It holds for all the plates with the hole and without a hole. The interesting point is that the nonlinear part after the elastic buckling happened, all the plates with and without holes resulted in almost the same buckling resistance. It can be concluded that for a specific thickness and boundary condition, perforating the hole does not significantly affect the post-buckling behavior of the plate.

c. Uniaxial and biaxial compression

Through this study, the buckling behavior of steel plates was investigated considering the uniaxial compression. In order to provide a comprehensive understanding of the buckling behavior of plates the biaxial in-plane compression was also studied and compared with

(a) Plate without hole

(b) Plate with hole (α=0.2)

(c) Plate with hole (α=0.4)
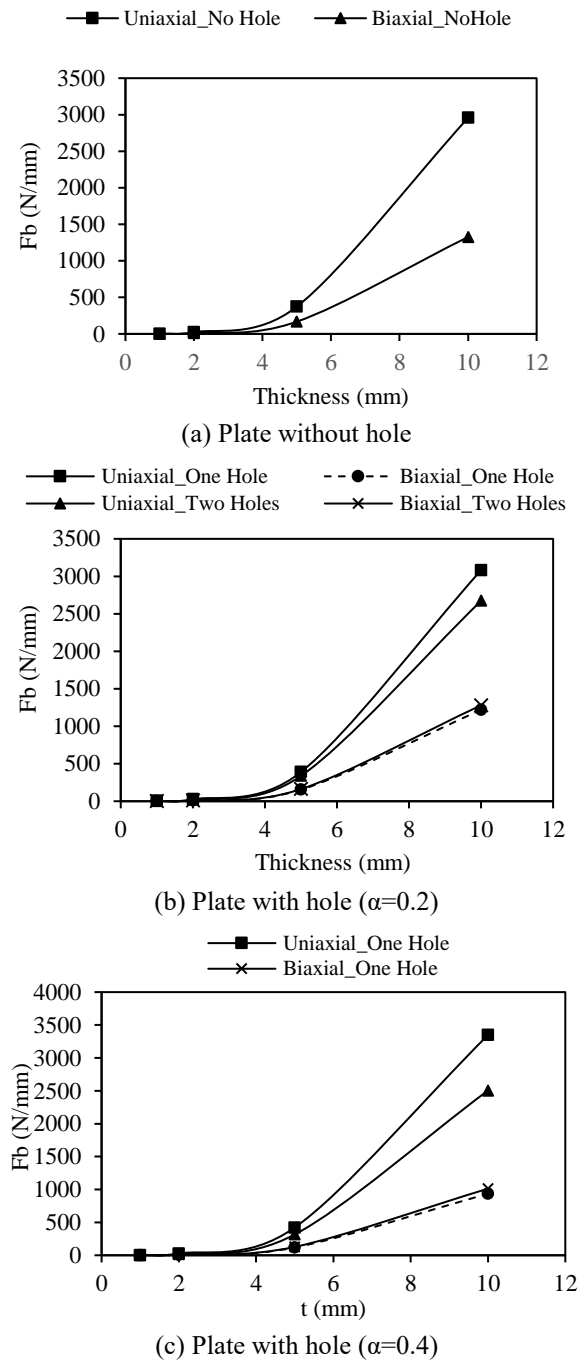
Fig. 14 Comparative graphs showing the variation of F_b with respect to h considering uniaxial and biaxial compression

F_b corresponding to uniaxial compression. For this aim, plates with holes utilizing the *AR= 0.5*, thicknesses of 1, 2, 5, and 10 mm and α=0.2, 0.4 were considered. The boundary conditions of the case *I* were applied to the plate. Fig. 14 illustrates the comparative graphs obtained for both cases of uniaxial and biaxial compression with respect to plate thickness.

As can be seen from the graphs given in Fig. 14 the plate under biaxial compression is less resistant to the buckling. The variation of F_b with respect to *h* showed that the trend in case of biaxial compression did not follow the

Fig. 15 Comparison between the buckling resistance of the plates subjected to uniaxial and biaxial compression

cubic pattern which obtained for the uniaxial compression. The buckling resistance of the plate increased with increasing the thickness but with a lower slope than the case of uniaxial compression.

For the case of uniaxial compression, it was found that perforating a hole at the plate center enhanced the buckling resistance of the plate while for the case of two holes the critical F_b decreased. The interesting point is that 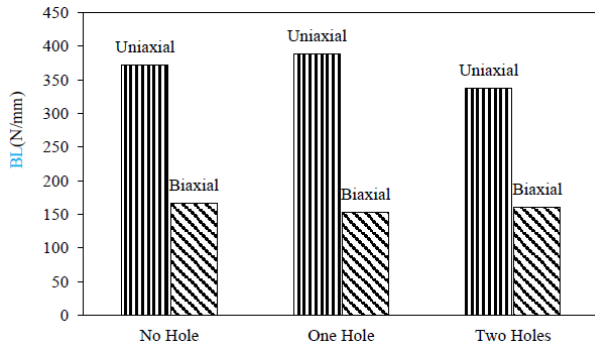for the case of biaxial compression perforating hole resulted in a decrease in critical F_b of the plate for both one and two holes. Besides, as can be observed from Figs. 14(b)-(c), both cases of plates with one hole and two holes provided approximately the same buckling resistance.

In order to provide a better understanding of the difference between the buckling resistance of the plate in case of uniaxial and biaxial compression, a comparative graph is provided in Fig. 15. It illustrates the maximum elastic F_b sustained by a plate of 5 mm thickness. For the plates with hole a hole diameter to the half the plate breadth of α=0.2 was considered.

Az can be observed in Fig. 15 the plate in case of biaxial compression is less buckling resistant about half of the case of uniaxial compression.

5. Conclusions

The investigations into the buckling behavior of plates with and without through-thickness holes were performed to provide a comprehensive study. For this aim, the commercially available finite element package ABAQUS was employed to carry out the analysis. The method was validated by comparing F_{br} obtained in this study and those given in the literature. Method validity proved that a good agreement was achieved. The effects of plate geometrical conditions, namely, h, AR, and imperfection on the plate buckling behavior was considered. Besides, the effects of perforating plate in the plate and hole Ecc were well studied together with considering four cases of plate boundary conditions. For the analysis, the uniaxial compression was considered. The results interestingly showed that perforating a hole at the plate center enhances the buckling resistance of the plate while perforating two holes resulted in a decrease in the critical load sustained by an aim plate. The investigation of the effects of boundary

condition on the plate buckling behavior showed that the case I for which the opposite side of the loading edge is fixed for all displacements and other edges were constrained only for out-of-plane displacement, can provide the best performance and resulted in the highest critical F_b. However, in case of having Ecc of holes the boundary condition of case IV for which the loading direction was free and plate lengths were fixed, showed the best performance and boundary condition of the case *I* did not yield to a good performance. For the plates with one hole, increasing Ecc in Y-direction resulted in a decrease in the critical F_b of the plate for both cases of boundary conditions while for plates with two holes no significant effect was observed when hole moves in Y-direction. The post buckling analysis showed that after the buckling occurred all plates with and without hole provide almost the same buckling resistance while before the buckling occurred the plate with one hole in the center, provided the highest buckling resistance. Investigation of subjecting biaxial compression proved that the plate buckling resistance substantially decreased lower than half of the case of uniaxial loading. It can be concluded that for design purposes it would be better to prevent the plate to be subjected to biaxial compression and or use some considerations such as using stiffeners to enhance the buckling performance of the plate. A comprehensive study of buckling behaviour of the biaxially loaded plates with and without holes can be performed as a future study.

References

Abdelbaki, C., Tounsi, A., Habib, H., Hassan, S. (2017), "Thermal buckling analysis of cross-ply laminated plates using a simplified HSDT", *Smart Struct. Syst.*, **19**(3), 289-297.

Abdelaziz, H.H., Meziane, M.A.A., Bousahla, A.A., Tounsi, A., Mahmoud, S.R., Alwabi, A.S. (2017), "An efficient hyperbolic shear deformation theory for bending, buckling and free vibration of FGM sandwich plates with various boundary conditions", *Steel Compos. Struct.*, **25**(6), 693-704.

Aghazadeh, R., Dag, S. and Cigeroglu, E. (2018), "Modeling of graded rectangular micro-plates with variable length scale parameters", *Struct. Eng. Mech.*, **65**(5), 573-585.

Akbas, S.D. (2014), "Large post-buckling behavior of Timoshenko beams under axial compression loads", *Struct. Eng. Mech.*, **51**(6), 955-971.

Aykac, B., Aykac, S., Kalkan, I. and Bocek, M. (2016), "The Out-of-plane bending behavior of brick infill wall strengthened with perforated steel plates", *Ingenieria, Investigaciony Tecnologia*, **17**(4), 429-435.

Bedair, O.K. (1997), "Influence of in-plane restraint on the buckling behaviour of plates under uniform compression, shear and in-plane bending", *Comput. Meth. Appl. Mech. Eng.*, **148**(1-2), 1-10.

Bedair, O.K. and Sherbourne, A.N. (1994), "On the stability of

plates under combined compression and in-plane bending", *Comput. Struct.*, **53**(6), 1453-1464.

Bouderba, B., Sid Ahmed, H.M., Tounsi, A. and Hassan, S. (2016), "Thermal stability of functionally graded sandwich plates using a simple shear deformation theory", *Struct. Eng. Mech.*, **58**(3), 397-422.

Bousahla, A.A., Benyoucef, S. and Tounsi, A. (2016), "On thermal stability of plates with functionally graded coefficient of thermal expansion", *Struct. Eng. Mech.*, **60**(2), 313-335.

Chajes, A. (1974), *Principles of Structural Stability Theory*, Prentice-Hall, Englewood Cliffs, New Jersey, U.S.A.

Timoshenko, S.P. and Gere, J.M. (2010), *Theory of Elastic Stability*, Tata McGraw-Hill Education Pvt. Ltd., New Delhi, India.

Choi, E., Mohammadzadeh, B., Kim, D. and Jeon, J.S. (2018), "A new experimental investigation into the effects of reinforcing mortar beams with superelastic SMA fibers on controlling and closing cracks", *Compos. Part B*, **137**, 140-152.

Choi, E., Mohammadzadeh, B., Hwang, J.H. and Kim, W.J. (2018), "Pullout behavior of superelastic SMA fibers with various end-shapes embedded in cement mortar", *Constr. Build. Mater.*, **167**, 605-616.

Choi, E., Chae, S.W., Park, H., Nam, T.H., Mohammadzadeh, B. and Hwang, J.H. (2018), "Investigating self-centering capacity of superelastic shape memory alloy fibers with different anchorages through pullout tests", *J. Nanosci. Nanotechnol.*, **18**(9), 6228-6232.

C.Scheperboer, I., Efthymiou, E. and and Maljaars, J. (2016), "Local buckling of aluminum and steel plates with multiple holes", *Thin-Wall. Struct.*, **99**, 132-141.

El-Hania, F., Bakora, A., Bousahla, A.A., Tunsi, A. and Mahmoud, S.R. (2017), "A simple analytical approach for thermal buckling of thick functionally graded sandwich plates", *Struct. Eng. Mech.*, **63**(5), 585-595.

El-Sawy, K.M. and Nazmy, A.S. (2001), "Effect of aspect ratio on the elastic buckling of uniaxially loaded plates with eccentric holes", *Thin-Wall. Struct.*, **39**(12), 983-998.

Guo, S., Li, D., Zhang, X. and Xiang, J. (2014), "Buckling and post-buckling of a composite C-section with cutout and flange reinforcement", *Compos. Part B: Eng.*, **60**, 119-124.

Hichem, B., Benrahou, K.H., Bousahla, A.A., Tounsi, A. and Hassan, S. (2017), "A nonlocal zeroth-order shear deformation theory for nonlinear postbuckling of nanobeams", *Struct. Eng. Mech.*, **62**(6), 695-702.

Jana, P. (2016), "Optimal design of uniaxially compressed perforated rectangular plate for maximum buckling load", *Thin-Wall. Struct.*, **103**, 225-230.

Jiao, P., Chen, Z., Xu, F., Tang, X. and Su, W. (2018), "Effects of ringed stiffener on the buckling behavior of cylindrical shells with cutout under axial compression: Experimental and numerical investigation", *Thin-Wall. Struct.*, **123**, 232-243.

Jowhari Moghadam, S. (2015), "Plastic buckling of columns and plats", Ph.D. Dissertation, Imperial College, London, U.K.

Kaci, A., Houari, M.S.A., Bousahla, A.A., Tounsi, A. and Mahmoud, S.R. (2018), "Post-buckling analysis of shear-deformable composite beams using a novel simple two-unknown beam theory", *Struct. Eng. Mech.*, **65**(5), 621-631.

Kasaeian, Sh., Azhari, M., Heidarpour, A. and Hajiannia, A. (2012), "Inelastic local buckling of curved plates with or without thickness-tapered sections using finite strip method", *Int. J. Steel Struct.*, **12**(3), 427-442.

Khetir, H., Bouiadjra, M.B., Sid Ahmed, H.M., Tounsi, A. and Hassan, S. (2017), "A new nonlocal trigonometric shear deformation theory for themal buckling analysis of embedded nanosized FG plates", *Struct. Eng. Mech.*, **64**(4), 391-402.

Kim, H.S., Park, Y.M., Kim, B.J. and Kim, K. (2018), "Numerical investigation of buckling strength of longitudinally stiffened web of plate girders subjected to bending", *Struct. Eng. Mech.*, **65**(4), 141-154.

Kim, J.H., Jeon, J.H., Park, J.S., Seo, H.D., Ahn, H.J. and Lee, J.M. (2015), "ㅊ, *Int. J. Mech. Sci.*, **92**, 194-205.

Kiran, M.C. and Kattimani, S.C. (2017), "Buckling characteristics and static studies of multilayered magneto-electro-elastic plate", *Struct. Eng. Mech.*, **64**(6), 751-763.

Komur, M.A. and Sonmez, M. (2015), "Elastic buckling behavior of rectangular plates with holes subjected to partial edge loading", *J. Constr. Steel Res.*, **112**, 54-60.

Komur, M.A. (2011), "Elasto-plastic buckling analysis for perforated steel plates subjected to uniform compression", *Mech. Res. Commun.*, **38**(2), 117-122.

Ko, W.L. (1998), *Mechanical- and Thermal-Buckling Behavior of Rectangular Plates with Different Central Cutouts*, Dryden Flight Research Center, Edwards, California, U.S.A., National Aeronautics and Space Administration.

Le Grognec, P. and Van., A.L. (2011), "On the plastic bifurcation and post-bifurcation of axially compressed beams", *Int. J. Non-Lin. Mech.*, **46**(5), 693-702.

Le Grognec, P. and Saoud, K.S. (2015), "Elastoplastic buckling and post-buckling analysis of sandwich columns", *Int. J. Non-Lin. Mech.*, **72**, 67-79.

Maiorana, E., Pellegrino, C. and Modena, C. (2009), "Elastic stability of plates with circular and rectangular holes subjected to axial compression and bending moment", *Thin-Wall. Struct.*, **47**(3), 241-255.

Menasria, A., Bouhadra, A., Tounsi, A., Bousahla, A.A. and Hassan, S. (2017), "A new and simple HSDT for thermal stability analysis of FG sandwich plats", *Steel Compos. Struct.*, **25**(2), 157-175.

Meziane, M.A.A., Abdelaziz, H.H. and Tounsi, A. (2014), "An efficient and simple refined theory for buckling and free vibration of exponentially graded sandwich plates under various boundary conditions", *J. Sandw. Struct. Mater.*, **16**(3), 293-318.

Mokhtar, Y., Heireche, H., Bousahla, A.A., Houari, M.S.A., Tounsi, A. and Mahmoud, S.R. (2018), "A novel shear deformation theory for buckling analysis of single layer graphene sheet based on nonlocal elasticity theory", *Smart Struct. Syst.*, **21**(4), 397-405.

Mohammadzadeh, B. and Noh, H.C. (2017), "Analytical method to investigate nonlinear dynamic responses of sandwich plates with FGM faces resting on elastic foundation considering blast loads", *Compos. Struct.*, **174**, 142-157.

Mohammadzadeh, B. and Noh, H.C. (2015), "Numerical analysis of dynamic responses of the plate subjected to impulsive loads", *Int. J. Civil, Environ., Struct., Constr. Architect. Eng.*, **9**(9), 1148-1151.

Mohammadzadeh, B., Bina, M. and Hasounizadeh, H. (2012), "Application and comparison of mathematical and physical models on inspecting slab of stilling basin floor under static and dynamic forces", *Appl. Mech. Mater.*, **147**, 283-287.

Mohammadzadeh, B. and Noh, H.C. (2014), "Investigation into central-difference and Newmark's beta method in measuring dynamic responses", *Adv. Mater. Res.*, **831**, 95-99.

Mohammadzadeh, B. and Noh, H.C (2016), "Investigation into buckling coefficients of plates with holes considering variation of hole size and plate thickness", *Mechan.*, **22**(3), 167-175.

Mohammadzadeh, B. and Noh, H.C. (2014), "Use of buckling coefficient in predicting buckling load of plates with and without holes", *J. Kor. Soc. Adv. Comp. Struct.*, **5**(3), 1-7.

Mohammadzadeh, B. and Noh, H.C. (2018), "An analytical and numerical investigation on the dynamic responses of steel plates considering the blast loads", *Int. J. Steel Struct.*

Musa, I.A. (2016), "Buckling of plates including effect of shear deformations: A hyperelastic formulation", *Struct. Eng. Mech.*, **57**(6), 1107-1124.

Nguyen, V.V., Hancock, G. J. and Pham, C.H. (2017), "Analysis of thin-walled sections under localized loading for general end boundary conditions-part 1: Pre-buckling", *Thin-Wall. Struct.*, **119**, 956-972.

Pham, C.H. (2017), "Shear buckling of plates and thin-walled channel sections with holes", *J. Constr. Steel Res.*, **128**, 800-811.

Prajapat, K., Ray-Chaudhuri, S. and Kumar, A. (2015), "Effect of in-plane boundary conditions on elastic buckling behavior of solid and perforated plates", *Thin-Wall. Struct.*, **90**, 171-181.

Ruocco, E., Mallardo, V., Minutolo, V. and Di Giacinto, D. (2017), "Analytical solution for buckling of Mindlin plates subjected to arbitrary boundary conditions", *Appl. Math. Modell.*, **50**, 497-508.

Sabir, A.B. and Chow, F.Y. (1986), "Elastic buckling of plates containing eccentrically located circular holes", *Thin-Wall. Struct.*, **4**(2), 135-149.

Sadamoto, S., Tanaka, S., Taniguchi, K., Ozdemir, M., Bui, T.Q., Murakami, C. and Yanagihara, D. (2017), "Buckling analysis of stiffened plate structures by an improved meshfree flat shell formulation", *Thin-Wall. Struct.*, **117**, 303-313.

Seifi, R., Chahardoli, S. and Akhavan Attar, A. (2017), "Axial buckling of perforated plates reinforced with strips and middle tubes", *Mech. Res. Commun.*, **85**, 21-32.

Shanley, F.R. (1946), "The column paradox", *J. Aeronaut. Sci.*, **13**(12), 678-678.

Shimizu, S. (2007), "Tension buckling of plate having a hole", *Thin-Wall. Struct.*, **45**(10-11), 827-833.

Soares, R.A. and Palermo Jr, L. (2017), "Effect of shear deformation on the buckling parameter of perforated and non-perforated plates studied using the boundary element method", *Eng. Analy. Bound. Elem.*, **85**, 57-69.

Sweedan, A.M.I. and Sawy, K.M. (2011), "Elastic local buckling of perforated webs of steel cellular beam-column elements", *J. Constr. Steel Res.*, **67**(7), 1115-1127.

Tajdari, M., Nezamabadi, A.R., Naeemi, M. and Pirali, P. (2011), "The effect of plate-support condition on buckling strength of rectangular perforated plates under linearly varying in-plane normal load", *World Acad. Sci. Eng. Technol.*, **54**, 479-486.

Degtyarev, V. and Degtyareva, N. (2017), "Numerical simulations on cold-formed steel channels with flat slotted webs in shear. Part I: Elastic shear buckling characteristics", *Thin-Wall. Struct.*, **119**, 22-32.

Xie, K., Chen, M. and Li, Z. (2017), "An analytic method for free and forced vibration analysis of stepped conical shells with arbitrary boundary conditions", *Thin-Wall. Struct.*, **111**, 126-137.

Xinwei, W. and Zhangxian, Y. (2018), "Buckling analysis of isotropic skew plates under general in-plane loads by the modified differential quadrature method", *Appl. Math. Modell.*, **56**, 83-95.

Yzid, M., Heirche, H., Tounsi, A., Anis, Bousahla, A.A. and Houari, M.S.A. (2018), "A novel nonlocal refined plate theory for stability response of orthotropic single-layer graphene sheet resting on elastic medium", *Smart Struct. Syst.*, **21**(1), 15-25.

Ziane, N., Meftah, S.A., Ruta, G., Tounsi, A. and Bedia, E.A.A. (2015), "Investigation of the instability of FGM box beams", *Struct. Eng. Mech.*, **54**(3), 579-595.

PL

Appendix: Buckling coefficient of plate with one hole

Aspect ratio	Thickness (mm)	α(d/a)							
		0.05	0.1	0.2	0.3	0.4	0.5	0.6	0.7
0.2	1	3.96	3.94	3.88	3.84	3.88	3.96	4.02	4.04
	2	3.95	3.93	3.87	3.83	3.86	3.95	4.01	4.02
	3	3.94	3.92	3.85	3.81	3.85	3.93	3.99	4.01
	4	3.92	3.90	3.84	3.80	3.83	3.92	3.97	3.99
	5	3.90	3.89	3.83	3.78	3.82	3.90	3.96	3.97
	6	3.89	3.87	3.81	3.77	3.80	3.88	3.94	3.95
	7	3.87	3.85	3.79	3.75	3.78	3.86	3.92	3.93
	8	3.85	3.83	3.78	3.73	3.76	3.84	3.90	3.91
	9	3.83	3.82	3.76	3.72	3.74	3.82	3.88	3.87
	10	3.53	3.53	3.53	3.52	3.49	3.44	3.34	3.13
0.3	1	3.99	3.97	3.88	3.83	3.87	3.99	4.10	4.13
	2	3.99	3.96	3.87	3.82	3.86	3.98	4.09	4.12
	3	3.98	3.95	3.86	3.81	3.85	3.97	4.08	4.11
	4	3.97	3.94	3.86	3.80	3.84	3.96	4.07	4.10
	5	3.96	3.93	3.84	3.79	3.83	3.95	4.06	4.09
	6	3.95	3.92	3.84	3.78	3.82	3.94	4.04	4.07
	7	3.94	3.91	3.83	3.77	3.81	3.92	4.03	4.06
	8	3.93	3.90	3.82	3.76	3.80	3.91	4.02	4.05
	9	3.92	3.89	3.81	3.75	3.79	3.90	4.00	4.03
	10	3.90	3.88	3.80	3.74	3.78	3.88	3.99	4.02
0.4	1	4.07	4.04	3.94	3.89	3.95	4.15	4.42	4.72
	2	4.06	4.03	3.93	3.88	3.95	4.13	4.41	4.71
	3	4.06	4.02	3.92	3.87	3.94	4.13	4.40	4.70
	4	4.05	4.02	3.92	3.87	3.93	4.12	4.39	4.69
	5	4.04	4.01	3.91	3.86	3.93	4.11	4.38	4.68
	6	4.03	4.00	3.90	3.85	3.92	4.10	4.36	4.67
	7	4.03	3.99	3.89	3.84	3.91	4.09	4.35	4.65
	8	4.02	3.98	3.88	3.84	3.90	4.07	4.34	4.64
	9	4.01	3.97	3.88	3.83	3.89	4.06	4.33	4.63
	10	4.00	3.97	3.87	3.82	3.88	4.05	4.31	4.61

Appendix: Buckling coefficient of plate with one hole

Aspect ratio	Thickness (mm)	$\alpha(d/a)$							
		0.05	0.1	0.2	0.3	0.4	0.5	0.6	0.7
0.5	1	3.95	3.99	4.12	4.31	4.48	4.77	5.24	5.90
	2	3.96	3.99	4.12	4.31	4.47	4.76	5.22	5.89
	3	3.95	3.99	4.11	4.30	4.47	4.75	5.21	5.88
	4	3.95	3.98	4.10	4.29	4.46	4.74	5.20	5.86
	5	3.94	3.97	4.10	4.28	4.45	4.73	5.18	5.84
	6	3.93	3.97	4.09	4.28	4.44	4.72	5.17	5.83
	7	3.93	3.96	4.08	4.27	4.44	4.71	5.15	5.81
	8	3.92	3.95	4.07	4.26	4.43	4.70	5.14	5.79
	9	3.91	3.95	4.07	4.25	4.42	4.69	5.12	5.77
	10	3.91	3.94	4.06	4.24	4.41	4.67	5.11	5.75
0.6	1	4.10	4.13	4.31	4.51	4.74	5.12	5.69	6.52
	2	4.09	4.13	4.29	4.51	4.73	5.11	5.67	6.49
	3	4.09	4.13	4.29	4.51	4.72	5.10	5.65	6.46
	4	4.08	4.12	4.28	4.50	4.71	5.09	5.63	6.43
	5	4.08	4.12	4.27	4.49	4.71	5.08	5.61	6.40
	6	4.07	4.11	4.27	4.48	4.70	5.06	5.59	6.37
	7	4.06	4.11	4.26	4.47	4.69	5.05	5.58	6.33
	8	4.06	4.10	4.25	4.47	4.69	5.04	5.56	6.30
	9	4.05	4.10	4.25	4.46	4.68	5.03	5.54	6.27
	10	4.05	4.09	4.24	4.45	4.67	5.02	5.52	6.23
0.7	1	4.39	4.36	4.18	4.10	4.21	4.57	5.16	6.09
	2	4.38	4.36	4.19	4.09	4.20	4.56	5.15	6.08
	3	4.38	4.35	4.18	4.09	4.20	4.56	5.13	6.05
	4	4.37	4.35	4.18	4.08	4.19	4.55	5.12	6.03
	5	4.37	4.34	4.17	4.08	4.19	4.54	5.10	6.00
	6	4.36	4.34	4.17	4.07	4.18	4.53	5.09	5.97
	7	4.36	4.33	4.16	4.07	4.18	4.52	5.07	5.95
	8	4.35	4.33	4.16	4.06	4.17	4.51	5.06	5.92
	9	4.35	4.32	4.15	4.06	4.16	4.50	5.04	5.90
	10	4.34	4.32	4.15	4.05	4.16	4.49	5.03	5.87

Aspect ratio	Thickness (mm)	$\alpha(d/a)$							
		0.05	0.1	0.2	0.3	0.4	0.5	0.6	0.7
0.8	1	4.11	4.01	3.84	3.71	3.78	3.98	4.32	4.75
	2	4.10	4.02	3.82	3.70	3.76	3.98	4.30	4.73
	3	4.09	4.02	3.82	3.70	3.75	3.98	4.29	4.71
	4	4.09	4.01	3.81	3.70	3.75	3.97	4.28	4.70
	5	4.08	4.01	3.81	3.69	3.74	3.96	4.27	4.68
	6	4.08	4.01	3.81	3.69	3.74	3.95	4.26	4.67
	7	4.07	4.00	3.80	3.68	3.73	3.95	4.25	4.65
	8	4.07	4.00	3.80	3.68	3.73	3.94	4.24	4.64
	9	4.07	3.99	3.79	3.67	3.72	3.93	4.23	4.62
	10	4.06	3.99	3.79	3.67	3.72	3.92	4.22	4.61
0.9	1	3.93	3.84	3.63	3.46	3.46	3.54	3.63	3.63
	2	3.93	3.85	3.62	3.46	3.44	3.44	3.62	3.60
	3	3.93	3.84	3.61	3.46	3.45	3.54	3.61	3.59
	4	3.92	3.84	3.61	3.45	3.44	3.53	3.60	3.58
	5	3.92	3.83	3.60	3.45	3.44	3.53	3.60	3.57
	6	3.91	3.83	3.60	3.45	3.43	3.52	3.59	3.56
	7	3.91	3.83	3.60	3.44	3.43	3.52	3.58	3.55
	8	3.91	3.82	3.59	3.44	3.42	3.51	3.57	3.54
	9	3.90	3.82	3.59	3.43	3.42	3.50	3.56	3.53
	10	3.90	3.81	3.59	3.43	3.41	3.50	3.56	3.52
1.0	1	3.90	3.79	3.53	3.32	3.27	3.27	3.16	2.90
	2	3.88	3.78	3.52	3.32	3.25	3.25	3.15	2.90
	3	3.88	3.78	3.51	3.32	3.25	3.24	3.15	2.90
	4	3.87	3.77	3.51	3.31	3.25	3.23	3.14	2.89
	5	3.87	3.77	3.50	3.31	3.24	3.23	3.13	2.88
	6	3.86	3.76	3.50	3.31	3.24	3.22	3.13	2.88
	7	3.86	3.76	3.50	3.30	3.23	3.22	3.12	2.87
	8	3.86	3.76	3.49	3.30	3.23	3.21	3.11	2.86
	9	3.85	3.75	3.49	3.30	3.22	3.21	3.11	2.85
	10	3.85	3.75	3.49	3.29	3.22	3.20	3.10	2.85